ELSEVIER

Journal of Electrostatics 43 (1998) 83–100

Journal of
ELECTROSTATICS

Theoretical analysis of linear stability of electrified jets flowing at high velocity inside a coaxial electrode

G. Artana[1], H. Romat*, G. Touchard

Laboratoire d'Etudes Aérodynamiques, Université de Poitiers, 40 Avenue du Recteur Pineau, 86022 Poitiers Cedex, France

Received 14 October 1996; received in revised form 31 July 1997; accepted 5 August 1997

Abstract

In this article we develop a temporal linear stability analysis of a circular electrified jet flowing inside a cylindrical coaxial electrode. The problem of a high-velocity jet going in a gaseous atmosphere is examined and we analyze the results in order to bring out the influence of the electrification, the surface tension, the velocity and other parameters on the stability of the jet. From this theory we finally state the changes in the breakup phenomena that are expected to be observed when electrifying these jets. © 1998 Elsevier Science B.V. All rights reserved.

Keywords: Electrohydrodynamics; Liquid jets; Electrified jets; Hydrodynamic stability; Dispersion relation

1. Introduction

Usually, liquid jets appear in industrial processes where it is desired to increase the surface/volume ratio of the liquid (combustion, chemical reactors, etc.) or to cover a target with a liquid in droplets form (painting, pesticide applications, ink jets printers, etc). The electrification of the jets has enabled a higher control of these processes as the electric forces may change the stability of the jet or the trajectory of the charged droplets created by the jet disintegration.

In nonelectrified jets, we can observe different regimes when increasing the jet velocity (Rayleigh regime, wind regimes and atomization) [1]. Though these regimes are quite different from each other, from all of them we can have a rough idea of the breakup process of the liquid jet into droplets by means of a linear stability analysis [2–8].

* Corresponding author. Tel.: 11 4145 3618; fax: 11 4945 3403; e-mail: lpmf@pmfsil.univ-poitiers.fr.

[1] Now at: Conicet-Dep. de Mecanica Aplicada, Facultad de Ingenieria, Universidad de Buenos Aires, Paseo Colon 850 (1063), Buenos Aires, Argentine.

PII S0304-3886(97)00163-0

The stability analysis is concerned with the development in space and time of infinitesimal perturbations in a given basic flow. As a function of the kind of perturbation imposed to the flow, two different problems, the spatial and the temporal ones, have been usually considered.

The spatial problem considers that the perturbation is applied in a certain region and it follows a given function in time. A special case of this problem is the signaling problem where a perturbation is periodically forced at a specific location. The development in Fourier series of this kind of perturbation gives components with real values of frequencies ω and their variation in space is obtained with the complex wave numbers $k(\omega) = k_r(\omega) + ik_i(\omega)$ deduced from the dispersion equation $D(k, \omega) = 0$. The temporal problem considers that the perturbation is applied to the flow in a certain region of the space at time equal to zero. The development in Fourier series of this kind of perturbation gives components with real values of the wave number k and their variation in time is obtained with the complex frequencies $\omega(k) = \omega_r(k) + i\omega_i(k)$, roots of the dispersion equation. In general, both analyses give the same information only when the conditions specified in Gaster's theorem are verified [9]. Otherwise, in most cases we cannot extrapolate results from one analysis to the other.

The spatial analysis has usually been used to describe the response or "receptivity of the flow" to different excitation frequencies. The downstream development of the perturbation is considered as a set of spatially growing waves of various frequencies. With this analysis, we can specify which are the amplifying waves, that is to say those whose amplitude increase from the source of perturbation, and which are the evanescent ones, those whose amplitude decrease. Among others, Melcher [10], Crowley [11–13] and Atten [14–15], have undertaken this analysis in electrified jets with the excitation frequency imposed by electric forces through coaxial electrodes.

A large part of previous research has also been devoted to the temporal theory, and one of the first work has been carried out by Rayleigh [16]. Other researchers starting from different hypotheses have studied the effect on the stability of the jet of a radial electric field [17–23] of an axial electric field [24, 25] or both [26, 27].

The temporal analysis appears to be quite important as it enables to predict if the flow is linearly stable (temporal growth rate positive) and to establish the interval of frequencies of the waves susceptible of being amplified in a signaling problem. Also, if there is no preferential excitation of the jet, the linear temporal stability appears to be a good tool to give the first approach of the breakup phenomena of an electrified liquid jet. For instance, the wavelength of the most unstable wave (the one with the highest growth rate) can be associated with the mean droplet diameter produced by the disintegration of the jet.

To our knowledge, most of the previous research has dealt with jets issuing from a nozzle at the Rayleigh regime (low velocity). In this situation a hypothesis usually accepted is that the effect of the surrounding atmosphere on the stability of the jet can be neglected. At high velocities this hypothesis is very strong, as the breakup phenomenon differs from the Rayleigh regime mainly because of the interaction of the liquid jet with the surrounding gas.

The stability analysis of high-velocity jets shows that the flow is unstable for waves with short wavelengths compared to jet radius and for waves with a large

growth rate compared to the ones of Rayleigh regimes. Hence, from a mathematical point of view some simplifications for long waves can no longer be valid for these regimes and most of the salient features of capillary instabilities (Rayleigh regime) are not preserved. Also, as the perturbation has a large growth rate the assumption of a liquid jet with the surface at constant potential must be analyzed carefully because of the rapid movement of the interface.

The effect of finite electrical conductivity on the instability of electrified jets has been studied by different authors [27–29]. These works shed light on the problems of low-velocity jets but it does not seem appropriate to extend their results to high-velocity jets.

In this work, we do not undertake this study and we limit ourselves to two simple ideal situations, the surface of the jet being an equipotential and the surface of the jet moving so rapidly that charge position on the jet surface is governed only by fluid motion.

As a summary, in this article we propose to undertake a linear temporal analysis of an electrified liquid jet flowing at high velocity inside a cylindrical coaxial outer electrode. We look for predictions in the two extreme electrical situations above cited and from these theoretical results we propose to obtain some insight on the breakup process of the jet.

2. Theoretical study

2.1. Problem description and assumptions

Let us consider a liquid jet flowing vertically downwards out from an injector and into a gas at room pressure. Depending on the velocity of the liquid, one obtains different kinds of jets. The one of interest here corresponds to the second wind regime or to the regime of atomization, that is to say for very high velocity (about 100 m/s). For these regimes the aspect of the jet looks like a pulverization shaped as a cone composed of sparse droplets in most of its volume, except in the region of its revolution axis where the density of the droplets is very high.

This jet flows through one coaxial cylindrical electrode brought to a certain potential that we will consider positive. The potential of the electrode V_0 is maintained constant and the injector is earthed (see Fig. 1). The analysis of stability is done with an infinite jet inside an infinite electrode.

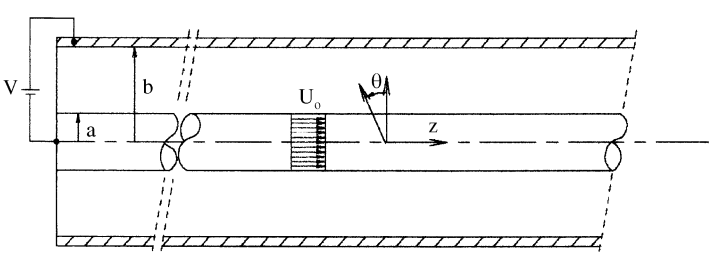

Fig. 1. Schema of the analyzed problem.

We assume the two fluids to be incompressible and the motion to be irrotational. We neglect the effects of gravity, magnetic fields, viscosity and mass transfer at the interface. Liquid and gas are considered as isothermal and incompressible and their electrical properties are those of an ohmic conductor for the liquid phase and of a perfect dielectric for the gaseous phase, both having uniform conductivity and dielectric constant. The electric charge on the jet is at the jet surface and there is no free charge source in the bulk of the liquid or of the gaseous phase. The velocity profile in a typical streamwise station is invariant with the axial co-ordinate.

2.2. The governing equations

To solve the problem we consider three regions: the regions of the liquid, gas and the interface. We use Gibbs's model [30] for the interface and we formulate the conservation equations as Slattery [31] and Philippe [32].

2.2.1. Fluid mechanics equations

The *mass conservation* leads to

– each phase

$$\boldsymbol{\nabla}\cdot\boldsymbol{U}_i = 0 \tag{1}$$

with $\boldsymbol{U}_i$ the velocity of the phase $i=1$ for the liquid and $i=2$ for the gas.

– at the interface

$$\nabla_\zeta\cdot\boldsymbol{U}_\zeta = 0, \tag{2}$$

where $\boldsymbol{U}_\zeta$ is the velocity vector of the interface and ∇_ζ the surface divergence.

The motion being irrotational we can consider a potential function for the velocity φ_i and we obtain the Laplace equation $\Delta\varphi_i = 0$.

As there is *no mass transfer* between phases

$$(\boldsymbol{U}_i - \boldsymbol{U}_\zeta)\cdot\boldsymbol{n} = 0, \tag{3}$$

or

$$(\boldsymbol{U}_1 - \boldsymbol{U}_2)\cdot\boldsymbol{n} = 0, \tag{4}$$

$\boldsymbol{n}$ being normal to the interface.

As for *momentum conservation*, it leads to

– in each phase:

$$\rho_{\mathbf{i}}\frac{\mathbf{d}\boldsymbol{U}_i}{\mathrm{d}t} - \nabla\circ\mathbf{T}_{\mathbf{i}} = \mathbf{0}. \tag{5}$$

$\rho_{\mathbf{i}}$ and $\mathbf{T}_{\mathbf{i}}$ are the mass density and Maxwell's constraint tensor of the phase $\mathbf{i}$ and

$$\frac{\mathrm{d}}{\mathrm{d}t} = \frac{\partial}{\partial t} + \boldsymbol{U}_i\cdot\nabla$$

is the material derivative.

– at the interface

$$-\nabla_\zeta \circ (\mathbf{T}_\zeta) - (\mathbf{T}_1 - \mathbf{T}_2) \circ \boldsymbol{n} = \mathbf{0}, \tag{6}$$

where $\mathbf{T}_\zeta$ is the constraint tensor in this region.

The expression of the Maxwell constraint tensor is $\mathbf{T_i} = -p_i\mathbf{I} + \mathbf{T}_\mathbf{i}^{el}$, where p_i is the static pressure and $\mathbf{I}$ the identity tensor [33]. The components of $\mathbf{T}_\mathbf{i}^{el}$, using Einstein's notation, are: $(T_i^{el})_{jk} = \varepsilon_i (E_i)_k (E_i)_j - (\varepsilon_i/2)\delta_{kj}(E_i)_m (E_i)_m$, with ε_i and $(E_i)_j$ the permittivity and the electric field in the jth direction, of the phase i. The expression of the surface constraint tensor is given by $\mathbf{T}_\zeta = \gamma_{i-j}(\mathbf{I} - \boldsymbol{n} \otimes \boldsymbol{n})$. According to [32]

$$\nabla_\zeta \circ \mathbf{T}_\xi = \gamma_{i-j}\langle \upsilon_n \rangle \boldsymbol{n} + \mathrm{grad}_\zeta \gamma_{i-j},$$

$\langle \upsilon_n \rangle$ being the mean curvature and γ_{i-j} the surface tension. As in our problem γ_{i-j} is constant, grad_ζ the surface gradient of this magnitude vanishes.

2.2.2. Electrical equations

We will use the Maxwell's equations simplified with our assumptions. In the bulk we can write [33]

$$\nabla \cdot \boldsymbol{D}_i = 0 \tag{7}$$

$$\nabla \times \boldsymbol{E}_i = \mathbf{0}, \tag{8}$$

here $\boldsymbol{E}_i$ and $\boldsymbol{D}_i$ are the electric field strength and the dielectric displacement.

By using an electrical potential function V, we express $\boldsymbol{E}_i = -\nabla V_i$ that leads to Laplace equation $\Delta V = 0$.

At the interface we will consider the continuity of the tangential electric field, Gauss law at the surface and conservation of charge considering the rate of change of a surface element are [34]

$$\boldsymbol{n} \times \| \boldsymbol{E}_i \| = \mathbf{0}, \tag{9}$$

$$\| \varepsilon_i \boldsymbol{E}_i \| \cdot \boldsymbol{n} = q_\zeta, \tag{10}$$

$$\frac{\mathrm{d}q_\zeta}{\mathrm{d}t} + q_\zeta (\boldsymbol{U}_\zeta \cdot \boldsymbol{n}) \nabla \boldsymbol{n} + \nabla_\zeta J_\zeta + \boldsymbol{n} \| J_i \| - (\boldsymbol{U}_\zeta \cdot \boldsymbol{n}) \| q_i \| = 0 \tag{11}$$

with q_ζ the surface charge, J_ζ the surface current density, J_i the volume current density, q_i the volume charge density and we notice a jump in a magnitude from a phase to another with the symbol $\| \|$.

2.3. The basic flow

The solution is expressed with the cylindrical coordinates r, θ and z in a referential R whose origin O is fixed to the center of the orifice of the injector moving with the axial jet velocity U_O. The z-axis is perpendicular to the plane containing the orifice of the injector whose radius is a, b being the radius of the electrode.

2.3.1. The velocity field of the nonperturbed jet

The velocity profile taken for the nonperturbed jet is $\boldsymbol{U}_1(r, \theta, z) = \boldsymbol{0}$ and $\boldsymbol{U}_2(r, \theta, z) = \boldsymbol{U}_0 = U_0(0, 0, -1)$, that is to say constant in all the liquid and in the gas. Physically, the velocity passes from $\boldsymbol{U}_0$ to $\boldsymbol{0}$ within the interface whose thickness is very small compared to a or b.

2.3.2. The electric field of the nonperturbed jet

In the nonperturbed case negative electrical charges are uniformly placed on the surface of the jet which is consequently isopotential. In the liquid media this leads immediately to $V_1(r, \theta, z) = 0$ and $\boldsymbol{E}_1(r, \theta, z) = -\nabla V_1 = \boldsymbol{0}$. In the gas, the resolution of Poisson equation $\Delta V_2 = 0$ with $V_2(a, \theta, z) = 0$ and $V_2(b, \theta, z) = V_0$, gives

$$V_2(r, \theta, z) = V_0 \frac{\ln(r/a)}{\ln(b/a)}.$$

The electric field is then

$$\boldsymbol{E}_2(r, \theta, z) = -\frac{V_0}{\ln(b/a)} \frac{\boldsymbol{i}_r}{r}.$$

2.4. The linear stability analysis

In fact, this nonperturbed state is totally ideal as it never occurs because of the high instability character of the flow and the many possible sources of perturbation like, for instance, the roughness of the orifice of the injector which induces modifications on the ideal velocity and potential.

We simulate the real phenomenon, by artificially perturbing the solution we have just described. Hence, we perturb the interface between the liquid and the gas and we determine the modifications induced on the velocity, the electrical potential and the pressure. The perturbation, which is arbitrary, is decomposed into a Fourier series and so can be considered as a set of small elementary waves propagating on the surface of the jet. As we consider a linear analysis we will accept that there is no interaction between the different modes (or waves) and so the analysis can be undertaken for each individual mode [35]. The amplitude of some of them can diminish and for others it can grow until it becomes large enough to give rise to droplets. Therefore, the study of the creation of the droplets boil down to the one of the stability of the jet submitted to a perturbation, whatever its origin.

Let us suppose that the flow is subjected to a modification at its interface. The coordinates of each point at the interface $\boldsymbol{OM}_\zeta = (a, \theta, z, t)$ become, $\boldsymbol{OM}_\zeta = (r_s(\theta, z, t), \theta, z)$ after modification. Where $r_s = a + \eta$, and η is the perturbation that depends on the space variables and on time t. Because we analyze the initial stages of growth or decay, we may analyze directly a single mode and η can be written as

$$\eta = \eta_0 \exp[(\omega t + \mathrm{i}(kz + n\theta))].$$

At the interface, the normal $\boldsymbol{n}$ to the interface at any point is $\boldsymbol{n} = (1, -(\mathrm{i}n/a)\eta, -\mathrm{i}k\eta)$ and the mean curvature $\langle \upsilon_n \rangle$ is

$$\langle \upsilon_n \rangle = \boldsymbol{V}\cdot\boldsymbol{n} = \frac{1}{r_s} - \frac{1}{r_s^2}\frac{\partial^2\eta}{\partial\theta^2} - \frac{\partial^2\eta}{\partial z^2}.$$

The perturbation of the interface leads to solutions for the velocity and for the electric field which are different from the ones obtained in the nonperturbed case. The governing equations of the fluid mechanics problem still are $\Delta\varphi_i = 0$ and $\Delta V_i = 0$ and we will have to solve them now with a moving interface (boundaries changing with time). Since we confine ourselves to the linear stability analysis, we will neglect all the terms proportional to η^2 or to higher exponents.

2.5. The perturbed state

2.5.1. Velocity field

Using Slattery's formulation [31] and considering that $\boldsymbol{U}_2(b, \theta, z) = \boldsymbol{0}$ and that the velocity is finite $\forall M$, we arrive to

$$\boldsymbol{U}_1 = C_1 \nabla(I_n(kr)\eta) \quad \text{and} \quad \boldsymbol{U}_2 = \boldsymbol{U}_0 + C_2 \nabla\left(\left(\frac{I_n(kr)}{C_3} + \frac{K_n(kr)}{C_4}\right)\eta\right)$$

with

$$C_1 = \frac{\omega}{kI_n'(ka)}, \quad C_2 = \frac{\omega - \mathrm{i}U_0 k}{k}, \quad C_3 = I_n'(ka)(1-\lambda) \quad \text{and} \quad C_4 = K_n'(ka)(1-1/\lambda)$$

with

$$\lambda = \frac{I_n'(kb)K_n'(ka)}{K_n'(kb)I_n'(ka)}.$$

I_n and K_n are the modified Bessels functions of first and second kind, I_n' and K_n' being their derivatives with respect to the variable r.

2.5.2. Electric field

The perturbed solution depends on the electrical state of the jet. Let us first remind that we perturb a cylindrical column of liquid flowing through a cylindrical coaxial electrode and that, in the nonperturbed state, the electrical charges are in electrical equilibrium on the surface of the liquid. The electrical state of the jet after perturbation depends on the way the electrical charges can move when the surface is perturbed. We consider two cases.

In the first one the electrical relaxation time of charges is small enough compared to a certain characteristic time of the deformation (in our case, the period of the perturbation). "Relexation is quicker than deformation". The jet remains isopotential at any time.

In the second case, which is the opposite extreme of the first one, the charges are in a way "linked" to the fluid particles and follow the dilatation and stretching of the

surface of the jet which consequently does not remain isopotential. This will be the case of jet with charges on its surface supporting a perturbation with a large growth rate (very high-velocity jet).

In what follows, we consider these two cases separately, it being understood that the reality of the electrical state of the surface is somewhere between them.

(a) *isopotential case*

If the surface of the liquid remains in electrical equilibrium despite the motion induced by the perturbation, the boundary conditions needed for the determination of the electric field in the gas are $V_2(b) = V_0$ at the electrode and $V_2(a+\eta) = 0$ at the interface.

Gauss law and the continuity of the tangential component of the electric field at the interface immediately give the solution in the liquid. We obtain

$$\boldsymbol{E}_1 = 0 \quad \text{and} \quad \boldsymbol{E}_2 = C_5 \nabla \left(\ln(r/a) - \left(\frac{I_n(kr)}{C_6} + \frac{K_n(kr)}{C_7} \right) \eta \right)$$

with

$$C_5 = \frac{V_0}{\ln(b/a)}, \quad C_6 = a\, I_n(ka)(1-\beta) \quad \text{and} \quad C_7 = a K_n(ka)(1-1/\beta),$$

being

$$\beta = \frac{K_n(ka) I_n(kb)}{I_n(ka) K_n(kb)}.$$

(b) *nonisopotential case*

As we have mentioned above, in this case we suppose that the electrical charges, uniformly distributed on the surface of the jet in the nonperturbed state, move by following the fluid particles of the surface. Now the distribution of the electrical charges on the surface of the jet is not uniform any longer.

From a physical point of view, the extremely rapid motion of the jet surface inhibits the rearrangement of the charges at the surface motivated by the electric forces. This assumption is equivalent to considering a problem in which the mobilities of the charges in the bulk and the interface are null.

So in the equation of charge conservation we can disregard any contribution of the current density in the rate of change of the surface charge density. The contribution of the surface current density is reduced to the convection term $\nabla_\zeta(q_\zeta \boldsymbol{U}_\zeta)$. However, as we only keep the linear terms, this convection term has no contribution either. The linearized equation can finally be written as

$$\frac{\partial q_\zeta}{\partial t} + q_\zeta (\boldsymbol{U}_\zeta \cdot \boldsymbol{n})\, \nabla \boldsymbol{n} = 0.$$

The integration in time of this equation then gives the following solution

$$q_\zeta(\theta, z, t) = q_0 \frac{a}{r_s},$$

where q_0 is the surface density of the electrical charges of the nonperturbed state ($t=0$).

The boundary conditions for the solution of Laplace equation that determines the value of the electric field are deduced from the following considerations:
– The potential at any point of the liquid (especially for $r=0$) is finite.
– In the gas we have $V_2(b)=V_0$.
– At the interface we use the traditional results deduced from Maxwell's equations: continuity of tangential component of the electric field and discontinuity of the normal component of the displacement vector.

Considering the electrical potential functions

$$V_i = A_i \ln(r/a) + R_i(r)\exp(\mathrm{i}(kz + n\theta) + \omega t) \quad \text{with } R_i(r) = B_{i1} I_n(kr) + B_{i2} K_n(kr)$$

and with the cited boundary conditions we have

$$\boldsymbol{E}_1 = C_5 \nabla\left(\frac{I_n(kr)}{C_8}\eta\right) \quad \text{and} \quad \boldsymbol{E}_2 = -C_5 \nabla\left(\ln(r/a) - \frac{K_n(kr)}{C_9}\eta\right)$$

with

$$C_8 = aI_n(ka)\left(1 - \frac{\varepsilon_1}{\varepsilon_2}\frac{I_n'(ka)K_n(ka)}{I_n(ka)K_n'(ka)}\right),$$

$$C_9 = aK_n(ka)\left(\frac{\varepsilon_2}{\varepsilon_1}\frac{K_n'(ka)I_n(ka)}{K_n(ka)I_n'(ka)} - 1\right),$$

ε_1 and ε_2 being the permittivities of the two media. In the expressions of the electric field in the gaseous phase we assume that the product kb is large enough to consider the quotient $K_n(kb)/I_n(kb) \approx 0$, condition usually verified.

2.5.3. *Pressure field*

Knowing the velocity and electric fields with the equation of conservation of linear momentum we determine the pressure in both media. The term $\mathrm{d}U_i/\mathrm{d}t$ can be written as

$$\frac{\mathrm{d}\boldsymbol{U}_i}{\mathrm{d}t} = \frac{\partial \boldsymbol{U}_i}{\partial t} + (\boldsymbol{U}_i \circ \nabla)\boldsymbol{U}_i,$$

where

$$(\boldsymbol{U}_i \circ \nabla)\boldsymbol{U}_i = (\nabla \times \boldsymbol{U}_i) \times \boldsymbol{U}_i + \tfrac{1}{2}\nabla(\boldsymbol{U}_i^2).$$

In our study, the motion is irrotational and the linearized Navier–Stokes equation then becomes

$$\rho_i \frac{\partial \boldsymbol{U}_i}{\partial t} = \nabla \circ (p_i \mathbf{I} + \mathbf{T}_{i_{e1}})$$

The solution of Navier–Stokes equation in terms of pressure is

$$p_1 = C_{10} I_n(kr)\eta \quad \text{and} \quad p_2 = C_{11} + C_{12}\left(\frac{I_n(kr)}{C_{13}} + \frac{K_n(kr)}{C_{14}}\eta\right)$$

with

$$C_{10} = -\rho_1 \frac{\omega^2}{kI_n'(ka)}, \quad C_{11} = -\rho_2 \frac{U_0^2}{2}, \quad C_{12} = -\rho_2 \frac{(\omega - \mathrm{i}U_0 k)^2}{k},$$

$$C_{13} = I_n'(ka)(1-\lambda) \quad \text{and} \quad C_{14} = K_n'(ka)(1-1/\lambda).$$

2.6. The dispersion equation

The dispersion equation is obtained by substitution of all terms in the momentum conservation equation at the interface. The equation we obtain is

$$\frac{\gamma_{i-j}}{\mathrm{a}^2} k(1 - n^2 - (ak)^2) + \rho_1 \frac{I_n(ak)}{I_n'(ka)}\omega^2 - \rho_2 \alpha \omega^2 (\omega - \mathrm{i}kU_0)^2$$

$$- \frac{\varepsilon_0 V^2}{a^3 \ln^2(b/a)} k(1 + ak\varsigma) = 0. \tag{12}$$

Considering a temporal analysis we can write

$$\omega_\mathrm{r}^2 = \frac{k}{a^2(1-\chi)\rho_2 \alpha}\left[-\gamma_{i,j}(1 - n^2 - (ak)^2) + \varepsilon_0 \frac{V^2}{a \ln^2(b/a)}(1 + ak\varsigma)\right] - \left(\frac{U_0 k}{1-\chi}\right)^2 \chi, \tag{13}$$

$$\omega_\mathrm{i} = \frac{U_0 k}{1-\chi}, \tag{14}$$

where

$$\chi = \frac{\rho_1 I_n(ak)}{\rho_2 I_n'(ak)\alpha} \quad \text{and} \quad \alpha = \frac{I_n(ka)}{I_n'(ka)(1-\lambda)} + \frac{K_n(ka)}{K_n'(ka)(1-1/\lambda)}$$

and where ω_r and ω_i are, respectively, the real part and the imaginary part of the growth rate ω.

In the equipotential case,

$$\varsigma = \frac{I_n'(ka)}{I_n(ka)(1-\beta)} + \frac{K_n'(ka)}{K_n(ka)(1-1/\beta)}$$

and in the nonequipotential one,

$$\varsigma = -\left(\frac{K_n(ka)}{K_n'(ka)} - \frac{\varepsilon_2 I_n(ka)}{\varepsilon_1 I_n'(ka)}\right)^{-1}.$$

These equations, taken in the same conditions as the ones of the articles of, respectively, Levich [2], Taylor [10], Melcher [19], Bailey [36], or Lin and Kang [37], give the same equation that each of these authors has found.

3. The results

In the next section, we determine the value of the corresponding ω for a given real wave number k and a given mode number n. If ω_r is positive, the jet is unstable and the greater ω_r is, the more unstable the jet is. On the other hand, if ω_r is negative or null then the jet is stable. As regards ω_i, we will just mention that $\partial\omega_i/\partial k$ is linked to the propagation velocity of the perturbation. In order to give an idea of the variation with ak we show some results in Section 3.1.

To better understand the physical consequences of the theoretical results we are going to present, it is useful to consult [2, 5, 38, 39] that deal with the breakup phenomena of high-velocity jets. In these works the authors established that the maximum $((\omega_r)_{max}, (k)_{max})$ of the curve $\omega_r(k)$ is related to the mean diameter $\bar{\Phi}$ of the first droplets, the angle Θ of the cone formed by the droplets, the intact length L_0 (the length of the jet before the detachment of the first droplet) and the breakup length (the length of the continuum jet) by

$$\bar{\Phi} = A\frac{2\pi}{(k)_{max}}, \quad \tan\left(\frac{\Theta}{2}\right) = B\frac{(\omega_r)_{max}}{(k)_{max}U_0}, \quad L_0 = \frac{C}{(\omega_r)_{max}}, \quad L_b = D\frac{k_{mx}}{\omega_{r_{mx}}}U_0$$

where A, B, C and D are experimental constants.

In the following figures, the parameters are fixed to 75 m/s for the velocity, to 72.2 mN/m for the surface tension, to 100 μm for the radius of the jet, to 20 μm for the radius of the electrode and to first mode $n=0$, except when we precisely study the influence of one of them.

3.1. Influence of the electrification on the stability of the jet

In Fig. 2(a), we have plotted the real part, ω_r, of the growth rate against the product ak (a being the radius of the orifice of the injector and k the wave number). In this figure, case 1 stands for nonelectrified jet, case 2 for electrified jet with surface at constant potential and case 3 for electrified jet with a nonequipotential surface. One can clearly see that each curve of that figure has a maximum. The abscissa of the

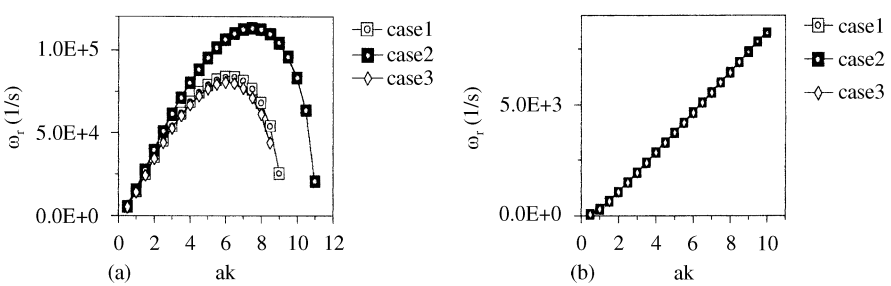

Fig. 2. (a) Influence of the electrification on the real part of the growth rate; (b) Influence of the electrification on the imaginary part of the growth rate.

maximum is related to the wavelength of the element of Fourier's decomposition ($k = 2\pi/\lambda$) which, in a linear approach, is supposed to give rise to the first droplets. Indeed, its growth rate being the greatest, this wave and those close to the maximum will grow more quickly than the others and predominate in the breakup process.

Now, let us compare the different cases of Fig. 1. Following the above explanation, the first droplets appear more rapidly, and are smaller in the equipotential case than in the other two cases (which are roughly identical). Consequently, these droplets are formed closer to the orifice of the injector in case 2 than in cases 1 and 3. The shape of the curves also tells us that, first the distribution of the size of all the droplets contains more droplets of small diameters in case 2 than in the two others and secondly the angle of the cone is more open in case 2 than in cases 1 and 3. It also tells us that the intact length and the breakup length are both shorter in case 2 than in cases 1 and 3.

In Fig. 2(b) we can see that the electrification has no significant influence on the evolution of the imaginary part ω_i of the growth rate. We will just point out that this means that the electric field has no influence on the propagation velocity of the perturbation on the surface of a high-velocity jet.

3.2. *Influence of the mode number on the stability of the jet*

Figs. 3 and 4, respectively, represent the influence of the mode in the equipotential and nonequipotential cases. The first and second mode ($n = 0$ and 1, respectively) are two modes whose behaviors are more or less the same: the curves are nearly superposed, and thus, the coordinates of the maximum of each mode are almost identical. The case $n = 2$ is a bit different from the latter two. The level of the rate of growth is slightly lower in the equipotential case but quite lower in the nonequipotential case. In both electrical cases, the coordinates of the maximum are smaller for $n = 2$ than for $n = 0$ and 1. These results mean that as we go further and further from the orifice of the injector, we can successively see droplets corresponding to the higher modes. This is more pronounced in the equipotential case than in the other.

In what follows, we will say that the influence of one parameter is destabilizing when for a fixed k or for a fixed range of k an increase in the value of the parameter

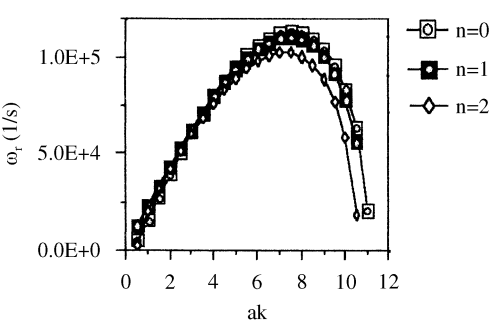

Fig. 3. Growth rate vs. ak for different mode number, equipotential case.

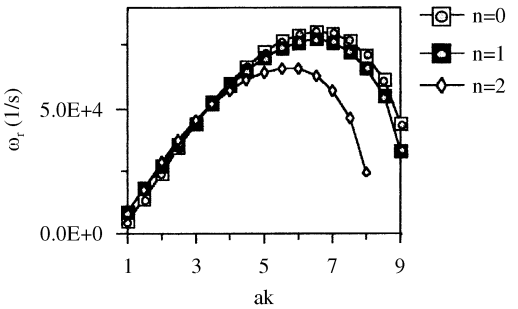

Fig. 4. Growth rate vs. *ak* for different mode number, nonequipotential case.

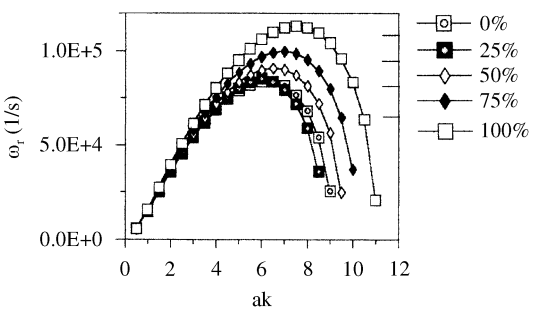

Fig. 5. Growth rate vs. *ak* for different intensities of the electric field.

causes an increase in the value of ω_r. The influence is destabilizing in the opposite case.

3.3. *Influence of the intensity of the electric field on the stability of the jet*

In Fig. 5 for the equipotential case we represent the variations of the growth rate vs. the product *ak* for different intensities of the electric field (from 0 to 100% of the intensity of the corona field). One can easily notice that as the electric field increases, the coordinates of the maximum of the corresponding curve increase too. Finally, the conclusion could be formulated as, the higher the intensity of the electric field the smaller the first droplets and the closer to the orifice of the injector they appear.

In order to complete this analysis we must look at the electrical term

$$\frac{k}{a^2(1-\chi)\rho_2\alpha}\,\varepsilon_0\,\frac{V^2}{a\ln^2(b/a)}\,(1+ak\varsigma)$$

of the dispersion equation. One can easily deduce that the electrical term is positive when $(1+ak\varsigma)<0$ and negative if it is greater than 0. The consequence of this, as

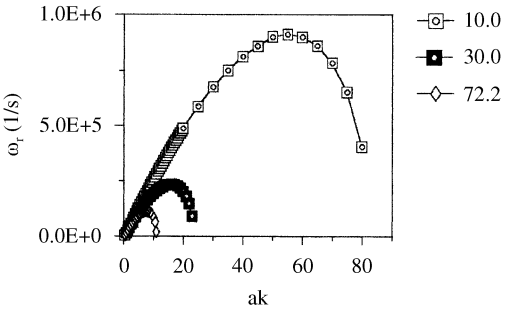

Fig. 6. Growth rate vs. *ak* for different values of the surface tension (mN/m).

one increases the electric field (here the electrical potential V) for a given wavelength, is that in the first case the solution ω_r of the dispersion equation also increases and in the second it diminishes. Thus, the electric field is respectively destabilizing and stabilizing. In Fig. 5, we are precisely in the case $(1 + ak\varsigma) < 0$ for the range of *ak* of interest (close to the maximum).

In the nonequipotential case, the results which we do not show here, prove that it is the other way round, the electric field is stabilizing for high-velocity jets for the range of *ak* of interest, that is to say $ak > 1$.

3.4. Influence of the surface tension on the stability of the jet

In Fig. 6 we report the results obtained in the equipotential case and for three values of the surface tension, 72.2 mN/m (water at room temperature), 10 and 30 mN/m (possible values for diesel oil). The influence of the surface tension is clear. The higher the surface tension, the bigger the first droplets and the further to the orifice of the injector they appear. Let us come back to the theory. In the dispersion equation, the term in which the influence of the interfacial tension is involved, is

$$-\frac{k}{a^2(1-\chi)\rho_2\alpha}\gamma_{i,j}(1-n^2-(ak)^2).$$

One can demonstrate that for high velocities for $ak > 1$, ω_r decreases with $\gamma_{i,j}$. The enhancement of the interfacial tension is then stabilizing, which is the case in Fig. 6. The radius-size distribution is now very different from one surface tension value to another, we will have many more small droplets with liquids whose surface tension is close to 10 (diesel oil, for example) than with liquids like water.

3.5. Influence of the radius of the jet on the stability of the jet

If we fix the electrical field (here 12.5 MV/m) and if we make the radius vary, all the other parameters being fixed too (except the potential which we must change as the

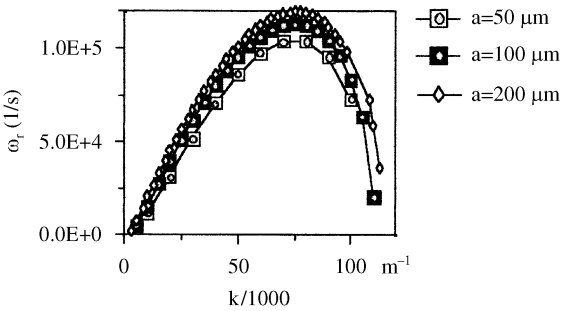

Fig. 7. Growth rate vs. wave number. Influence of the radius of the jet.

radius changes in order to have the electric field constant), we obtain the results reported in Fig. 7. The abscissa of the maxima does not change in the three cases considered here, but the corresponding ω_r coordinate increases with the radius. Physically this means that, at constant electric field, the radius of the orifice of the injector does not influence the size of the first droplets (nor even probably the distribution of the sizes of all the droplets because of the similarity of the shape of the three curves), but as the radius of the orifice of the injector increases (the one of the electrode remaining constant) the intact length L_0 of the jet diminishes slightly. The influence of the radius is thus destabilizing.

For a fixed potential, instead of a fixed electric field, the results not reported here, show that the level of ω_r is much higher for 50 μm than for 100 or 200 μm, which means that the influence of the radius is then stabilizing. Also, those results indicate that the k-coordinate of the maximum is higher for 50 μm than the two others for 100 and 200 μm. Thus, at constant potential, the size distribution of all the droplets changes, the spray will have a lot more droplets of small radii.

3.6. Influence of the velocity on the stability of the jet

In Fig. 8 we have the results concerning the influence of the velocity for the equipotential case. From it we can say that increasing the velocity diminishes the size of all the droplets and gives higher growth rates. More specifically, we notice that the first droplets are smaller and closer to the injector for high velocities than for low velocities: when we increase the velocity we destabilize the jet and we change the droplet-size distribution. For high velocities, the atomization starts closer to the injector and the jet contains droplets much smaller than for small velocities.

Figs. 9 and 10 give information on the influence of the electrification on the maxima of the curves (ω_r, ak) for different velocities. For extremely high velocities there is basically no influence of the electrification and the inertial forces are dominant. As a result no significant change is expected in droplet diameter when electrifying an extremely high velocity jet.

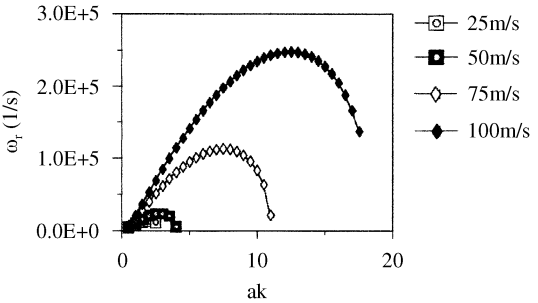

Fig. 8. Growth rate vs. *ak*. Influence of the jet velocity.

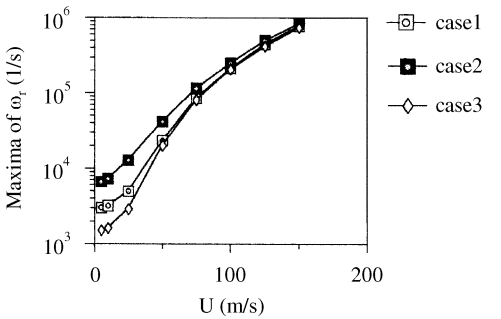

Fig. 9. Influence of the velocity on the maxima of the real part of the growth rate.

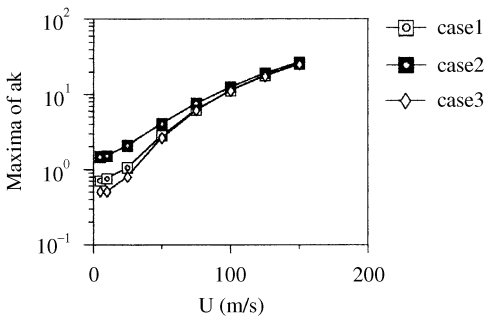

Fig. 10. Influence of the velocity on the maxima of *ak*.

4. Conclusion

We solved the dispersion equation for different values of the parameters to determine their influence on the stability of an electrified jet flowing at high velocity in a gaseous atmosphere.

The first important thing that we showed is that the electrification acts on the stability of a jet in a different way depending on the electrical state of the surface of the jet. The response is not the same whether the surface is considered equipotential or nonequipotential.

For the equipotential situation, an increase in the velocity or in the electric field or a decrease in the interfacial tension destabilizes the jet. This leads to more dispersed sprays with smaller droplets when the electric field and the velocity are high and when the interfacial tension is small. Besides as the intact and breakup lengths are smaller, the electrified jet will disintegrate closer to the injector, i.e. in a shorter distance from the nozzle.

For the situation of "frozen" charges on the jet surface, the effect of the electric field is opposed to the equipotential case. As a result for extremely high-velocity jets when the electrical relaxation time is much longer than the mechanical time constant, the charges on the surface stabilize the jet.

The difference in both cases can be explained by the distribution of the surface charge density. In the equipotential case for high-velocity jets, the surface-charge density is higher at the points of longer radii and the electric forces promote the enhancement of the instability. In the nonequipotential case, the redistribution of the charge caused by the electric forces is not achieved, and the charge is concentrated at the points with smaller radii, promoting the recuperation of the cylindrical shape that is to say dampening the instability of the jet.

When considering experimental arrangements with finite electrode lengths, as the jet velocities are high, the time the wave packages interacts with the electric field may be small because of the convective character of the instability. This problem requires a more detailed analysis and is not under the scope of this article. However, it should be pointed out that for high-velocity jets, the maximum of the growth rate is very important and the electric field in a very short time amplifies a wave different from the one of the nonelectrified jet. So, in this approach, though velocities are high we expect that the electric field will be "felt" by the jet and produce the cited modifications of the breakup process.

Acknowledgements

This paper relates a part of G. Artana's Doctoral Thesis which Dr. H. Romat and Prof. G. Touchard directed together at the University of Poitiers with the help of Dr. P. Atten to whom our thanks are due.

References

[1] R. Reitz, F. Bracco, Mechanisms of breakup of round liquid jets, Encyclopedia of Fluid Mechanics, NJ, Vol. 3, 1986, p. 233.
[2] V. Levich, Physicochemical Hydrodynamics, Prentice-Hall, Englewood Cliffs, NJ, 1962.
[3] M. McCarthy, N. Molloy, Review of stability of liquid jets and the influence of nozzle design, Chem. Eng. J. 7 (1974) 1.

[4] A. Sterling, C. Sleicher, The instability of capillary jets, J. Fluid Mech. 68 (3) (1975) 477.
[5] R. Reitz, F. Bracco, Mechanisms of atomization of a liquid jet, Phys. Fluids 25 (10) (1982) 1730.
[6] J. Martinon, Stability of a capillary cylindrical jet in an external flow, J. Appl. Math. Phys. 34 (1983) 575.
[7] G. Bower et al., Physical mechanisms for atomization of a jet spray: a comparison of models and experiments, SAE paper No. 881318.
[8] N. Chigier, The physics of atomization, ICLASS-91, Gaithersburg, 1991, p. 1.
[9] M. Gaster, A note on the relation between temporally increasing and spatially increasing disturbances in hydrodynamic stability, J. Fluid Mech. 14 (1962) 222.
[10] J. Melcher, Field Coupled Surface Waves, MIT Press, Cambridge, 1963.
[11] J. Crowley, Growth and excitation of electrohydrodynamique surface waves, Phys. Fluids 8 (9) (1965) 1668.
[12] J. Crowley, Ink jet electrohydrodynamic excitor, US Patent 4 220 958, 1980.
[13] J. Crowley, Electrohydrodynamic droplet generators, J. Electrostat. 14 (1983) 121.
[14] A. Spohn, P. Atten, EHD multi-electrode simulation of a conducting capillary jet, IEEE IAS Annual Meeting 1993, p. 1960.
[15] P. Atten et al., Electrohydrodynamic induction of isolated drops in a jet, I. P. Conf. Ser. 143 (1995) 47.
[16] F. Rayleigh, On the instabilities of jets, Proc. Lond. Math. Soc. 11 (1878) 4.
[17] A. Basset, Waves and jets in a viscous liquid, Amer. J. Math. 16 (1894) 93.
[18] J. Schneider et al., Stability of an electrified liquid jet, J. Appl. Phys. 38 (6) (1967) 2599.
[19] G. Taylor, Electrically driven jets, Proc. Roy. Soc. A 313 (1969) 453.
[20] A. Huebner, H. Chu, Instability and breakup of charged liquid jets, J. Fluid Mech. 49 (2) (1971) 361.
[21] A. Neukermans, Stability criteria of an electrified liquid jet, J. Appl. Phys. 44 (10) (1973) 4769.
[22] R. Turnbull, On the instability of an electrostatically sprayed liquid jet, IEEE IAS Annual Meeting, Seattle, 1990, p. 783.
[23] F. Garcia, A. Castellanos, Effect of interfacial electrical stresses on the stability of viscous liquids jets, I. P. Conf. Ser. 143 (1995) 301.
[24] N. Nayar, G. Murty, The stability of a dielectric liquid in the presence of a longitudinal electric field, Proc. Phys. Soc. London 75 (1960) 369.
[25] D. Saville, Electrohydrodynamic stability: fluid cylinders in longitudinal electric fields, Phys. Fluids 13 (12) (1970) 2987.
[26] J. Melcher, E. Warren, Electrohydrodynamics of a current carrying semi-insulating jet, J. Fluid Mech. 47 (1) (1971) 127.
[27] A. Mestel, Electrohydrodynamic stability of a slightly viscous jet, J. Fluid Mech. 274 (1994) 93.
[28] D. Saville, Electrohydrodynamic stability: effects of charge relaxation at the interface of the liquid, J. Fluid Mech. 48 (4) (1971) 815.
[29] R. Turnbull, Finite conductivity effects on electrostatically sprayed liquid jets, IEEE Trans. Ind. Appl. 32 (4) (1996) 837.
[30] J. Gibbs, The Collected Works of J. Gibbs, Vol. 1, Yale University Press, New Haven, CT, 1990.
[31] Slattery, Interfacial transport phenomena, Chem. Eng. Commun. 4 (1980) 149.
[32] C. Philippe, Thése de Doctorat, University of Poitiers, 1986.
[33] L. Landau, E. Lifchitz (Eds.), Physique Théorique, Tome VIII, MIR, Moscou, 1990.
[34] A. Castellanos, Nonlinear waves and instabilities on electrified free surfaces, ICDL96, Rome, 1996, p. 25.
[35] P. Drazin, H. Reid, Hydrodynamic Stability, Cambridge University Press, New York, 1981.
[36] A. Bailey, Electrostatics Spraying of Liquids, Wiley, New York, 1988.
[37] S. Lin, D. Kang, Atomisation of a liquid jet, Phys. Fluids 30 (7) (1987) 2000.
[38] W. Ranz, Some experiments on orifice sprays, Can. J. Chem. Eng. (1958) 175.
[39] K. Wu et al., Measurements of drop sizes at the spray edge near the nozzle in atomizing liquid jets, Phys. Fluids 29 (4) (1986) 941.